

## Rapidity dependent strangeness measurements in BRAHMS experiment at RHIC

J H Lee<sup>1</sup> (for the BRAHMIS Collaboration)

I G Bearden<sup>7</sup>, D Beavis<sup>1</sup>, C Besliu<sup>10</sup>, B Budick<sup>6</sup>, H Bøggild<sup>7</sup>, C Chasman<sup>1</sup>, C H Christensen<sup>7</sup>, P Christiansen<sup>7</sup>, J Cibor<sup>3</sup>, R Debbe<sup>1</sup>, E Enger<sup>12</sup>, J J Gaardhøje<sup>7</sup>, M Germinario<sup>7</sup>, K Hagel<sup>8</sup>, O Hansen<sup>7</sup>, A Holm<sup>7</sup>, H Ito<sup>11</sup>, E Jakobsen<sup>7</sup>, A Jipa<sup>10</sup>, F Jundt<sup>2</sup>, J I Jørdre<sup>9</sup>, C E Jørgensen<sup>7</sup>, R Karabowicz<sup>4</sup>, E J Kim<sup>1</sup>, T Kozik<sup>4</sup>, T M Larsen<sup>12</sup>, J H Lee<sup>1</sup>, Y K Lee<sup>5</sup>, G Løvhøiden<sup>12</sup>, Z Majka<sup>4</sup>, A Makeev<sup>8</sup>, M Mikelsen<sup>12</sup>, M Murray<sup>8</sup>, J Natowitz<sup>8</sup>, B S Nielsen<sup>7</sup>, J Norris<sup>11</sup>, K Olchanski<sup>1</sup>, J Olness<sup>1</sup>, D Ouerdane<sup>7</sup>, R Planeta<sup>4</sup>, F Rami<sup>2</sup>, C Ristea<sup>10</sup>, D Röhrich<sup>9</sup>, B H Samset<sup>12</sup>, D Sandberg<sup>7</sup>, S J Sanders<sup>11</sup>, P Staszal<sup>7</sup>, T S Tveter<sup>12</sup>, F Videbæk<sup>1</sup>, R Wada<sup>8</sup>, A Wieloch<sup>4</sup>, Z Yin<sup>9</sup> and I S Zgura<sup>10</sup>

<sup>1</sup> Physics Department, Brookhaven National Laboratory, Upton, New York 11973, USA

<sup>2</sup> Institut de Recherches Subatomiques and Université Louis Pasteur, Strasbourg, France

<sup>3</sup> Institute of Nuclear Physics, Krakow, Poland

<sup>4</sup> Smoluchowski Inst. of Physics, Jagiellonian University, Krakow, Poland

<sup>5</sup> Johns Hopkins University, Baltimore 21218, USA

<sup>6</sup> New York University, New York 10003, USA

<sup>7</sup> Niels Bohr Institute, Blegdamsvej 17, University of Copenhagen, Copenhagen 2100, Denmark

<sup>8</sup> Texas A&M University, College Station, Texas, 17843, USA

<sup>9</sup> University of Bergen, Department of Physics, Bergen, Norway

<sup>10</sup> University of Bucharest, Romania

<sup>11</sup> University of Kansas, Lawrence, Kansas 66049, USA

<sup>12</sup> University of Oslo, Department of Physics, Oslo, Norway

Received 18 June 2003

Published 11 December 2003

Online at [stacks.iop.org/JPhysG/30/S85](http://stacks.iop.org/JPhysG/30/S85) (DOI: 10.1088/0954-3899/30/1/007)

### Abstract

Particle production of charged kaons in central Au+Au collisions at  $\sqrt{s_{NN}} = 200$  GeV has been studied as a function of rapidity by the BRAHMS collaboration at RHIC. The kaon spectral shapes are described well by an exponential in transverse mass for the rapidity range of  $0 \leq y_K \leq 3.3$  with smoothly decreasing inverse slopes as the rapidity increases. For the charged kaon to pion ratios, while there is no significant rapidity dependence for the  $K^+/\pi^+$  ratio, the  $K^-/\pi^-$  ratio shows a significant decrease from  $y \approx 1$  towards higher rapidities. The systematics of  $K^-/K^+$  and  $\bar{p}/p$  ratios in the measured rapidity range demonstrates a strongly correlated behaviour which can be described by thermal–statistical models.

## 1. Introduction

Since the absolute yields and ratios of the strange particle abundances depend sensitively on the dynamics of the collision, strangeness production is of great interest in relativistic heavy-ion collision studies. The interest in these studies is particularly derived from the understanding that the strangeness production arises rapidly in the deconfined and chirally symmetric phase (QGP) created by the collisions [1, 2]. A number of experiments at AGS [3–5] and at SPS [6, 7] have shown that the strange particle abundance differs considerably in nucleus–nucleus interactions from that in nucleon–nucleon collisions.

Understanding the mechanism responsible for the enhancement has been a challenging subject theoretically since the enhancement expected from the chirally restored state can also be described by calculations for strangeness production based on hadronic and partonic mechanisms without assuming a phase transition [8–10]. In order to be able to be more specific about the nature of the strangeness production in heavy-ion collisions, it is imperative to study the strangeness production in a wide kinematic range ( $y$ – $p_T$ ) to constrain the theoretical models.

The relativistic heavy-ion collider (RHIC) permits the study of highly excited nuclear matter in the extreme high energy regime ( $\sqrt{s_{NN}} = 200$  GeV), energy of an order of magnitude higher than previously available energy at SPS. Studying strangeness production at this energy in the context of strangeness enhancement by comparing with measurements from lower energy data and with theoretical predictions will give dynamical information of the nature of the excited matter.

## 2. Experimental set-up

The BRAHMS (broad range hadron magnetic spectrometers) experiment [11] measures identified charged hadrons including kaons in a broad kinematic range at RHIC. The experiment consists of two movable spectrometers: the mid-rapidity spectrometer (MRS) and the forward spectrometer (FS), with the latter having independently movable front (FFS) and back (BFS) sections. The data collected with the BRAHMS detectors is in the rapidity range  $-0.1 < y < 3.5$ , an extended range unique among the RHIC experiments. The MRS determines particle momenta using two time projection chambers (TPC) and a dipole magnet. Particle identification is obtained using a time-of-flight (TOF) counter, with time resolution  $\sigma_t \approx 75$  ps allowing  $\pi$ –K separation up to a particle momentum ( $p$ ) of 2.3 GeV/ $c$  and K–p separation up to 3.9 GeV/ $c$ . The FFS consists, in order, of a dipole magnet, a TPC, a second dipole magnet, a second TPC, a TOF wall (TOF1) and a threshold gas-Cherenkov detector (C1). At the small polar angles (from  $2.3^\circ$  to  $15^\circ$ ), where the mean momentum of particles is large, the BFS with two dipole magnets, three drift chambers, a TOF wall (TOF2) and a ring imaging Cherenkov detector (RICH) is also used. TOF1 (at 8.6 m) and TOF2 (at 18 m) allow for K–p separation up to 5.5 and 8 GeV/ $c$ , respectively. C1 identifies pions in the range from  $p = 3$  to 9 GeV/ $c$  and the RICH allows  $\pi$ –K separation up to 22 GeV/ $c$  and K–p separation from  $p = 10$  to  $p = 35$  GeV/ $c$  [15]. The reaction centrality was determined using a multiplicity array which consists of plastic scintillator tiles and modestly segmented silicon strip detectors surrounding the intersection region [14]. More detailed description of the BRAHMS detectors can be found in [11].

The data set for charged kaons used for this analysis covers  $-0.05 \leq y \leq 1.1$  using the MRS, and  $2.1 \leq y \leq 3.3$  using the FS. Only the 0–5% most central events [14] were included in the analysis. Details on the data analysis can be found in [12].

### 3. Results and discussions

Figure 1 shows the transverse mass ( $m_T$ ) spectra for the invariant yields of positive and negative charged kaons at different rapidities ( $y$ ) in  $0 < y_K < 3.3$  where  $m_T = \sqrt{p_T^2 + m_K^2}$  and  $m_K$  is the kaon mass. The spectral shapes can be well represented by an exponential distributions  $[e^{-(m_T - m_K)/T}]$  with an inverse slope ( $T$ ) as indicated by the solid lines. The  $K^+$  spectra show similar slopes and yields to the  $K^-$  spectra. For comparison,  $m_T$  spectra for charged pions also shown in the figure with overlaid power-law  $[A(1 + p_T/p_0)^{-n}]$  fits. The error shown on the data points are statistical only. The overall systematic errors are estimated to be 10–15%.

Figure 2 shows the deduced inverse slope parameters  $T$  as a function of rapidity for kaons and pions. The kaon inverse slope parameter with values of  $295 \pm 4$  MeV for  $K^+$  and  $295 \pm 5$  MeV for  $K^-$  are almost constant at mid-rapidity. These values are significantly higher than found at SPS measurements ( $T_K \sim 230$  MeV). This may suggest a stronger radial flow and/or a systematic increase of the thermal temperature at the RHIC energy. The inverse slope parameters decrease at larger rapidities, implying the degree of radial flow decreases moving away from mid-rapidity. The inverse slope parameters at forward rapidity,  $y_K = 3.3$ , are fitted as  $245 \pm 9$  MeV for  $K^+$  and  $229 \pm 8$  MeV for  $K^-$ , which are close to the SPS mid-rapidity values. Mean transverse momenta ( $\langle p_T \rangle$ ), deduced from fitting the spectra, as a function of rapidity are also shown in figure 2. Kaons show a stronger rapidity dependence of  $T$  and  $\langle p_T \rangle$  than pions.

Rapidity density distributions,  $dN/dy$ , for charged kaons and pions are shown in figure 3. The total yields of  $286 \pm 11$  for  $K^+$  and  $236 \pm 8$  for  $K^-$  for 0–5% central events are determined by fitting the rapidity spectra with a sum of two Gaussian distributions placed symmetrically with respect to mid-rapidity. The width of the rapidity density for  $K^+$  is significantly wider than that for  $K^-$ . While  $dN/dy$  for  $\pi^-$  gets narrower as the collision energy increases, as shown in figure 4, there are no significant changes in the width of the  $dN/dy$  distribution for  $K^+$  between the top SPS energy and the RHIC energy.

The rapidity dependence of the  $K/\pi$  ratios are displayed in figure 5. While the  $K^+/\pi^+$  ratio is nearly constant in the rapidity range of  $|y_K| < 3.3$ , the  $K^-/\pi^-$  ratio shows a significant decrease from  $y \approx 1$  towards higher rapidity. Near mid-rapidity,  $|y_K| < 1$ , the  $K/\pi$  ratios are measured as  $0.156 \pm 0.001$  for  $K^+/\pi^+$  and  $0.146 \pm 0.001$ .

Mid-rapidity and full phase space kaon to pion ratios are shown as a function of  $\sqrt{s_{NN}}$  in figure 6. A monotonic increase with  $\sqrt{s_{NN}}$  of the  $K^-/\pi^-$  ratio is measured while  $K^+/\pi^+$  behaves differently. A steep increase in the low energy region is followed by a maximum around the lowest SPS energy,  $\sqrt{s_{NN}} = 8.8$  GeV. The measurement at RHIC suggests that the  $K^+/\pi^+$  ratio stays nearly constant starting from the top SPS energy.

Anti-particle to particle ratios for charged kaons,  $K^-/K^+$ , as a function of rapidity can be deduced from their rapidity densities [15]. At mid-rapidity ( $|y| < 1$ ), the ratio is close to unity ( $\sim 0.95$ ), which is a significant increase from the top SPS energy ( $\sim 0.6$ ). The ratio decreases with rapidity, and approaches to the SPS mid-rapidity values at  $y \sim 3$ . This rapidity dependence can be attributed to a sensitivity to the baryonic density. At the energy of  $\sqrt{s_{NN}} = 200$  GeV considerable reaction transparency is achieved for collisions [13], and away from mid-rapidity the net baryon content originating from the initial nuclei is significant and production mechanisms other than particle–antiparticle pair production play a significant role. This can lead to a decreasing  $K^-/K^+$  ratio with increasing rapidity. It has to be noted that theoretical models [16, 17] that are relatively successful in reproducing multiplicity distributions [14] and rapidity dependent anti-particle to particle ratios for protons and pions ( $\bar{p}/p$ ,  $\pi^-/\pi^+$ ) [15] fail to describe the rapidity dependent  $K^-/K^+$  ratios at the RHIC energies.

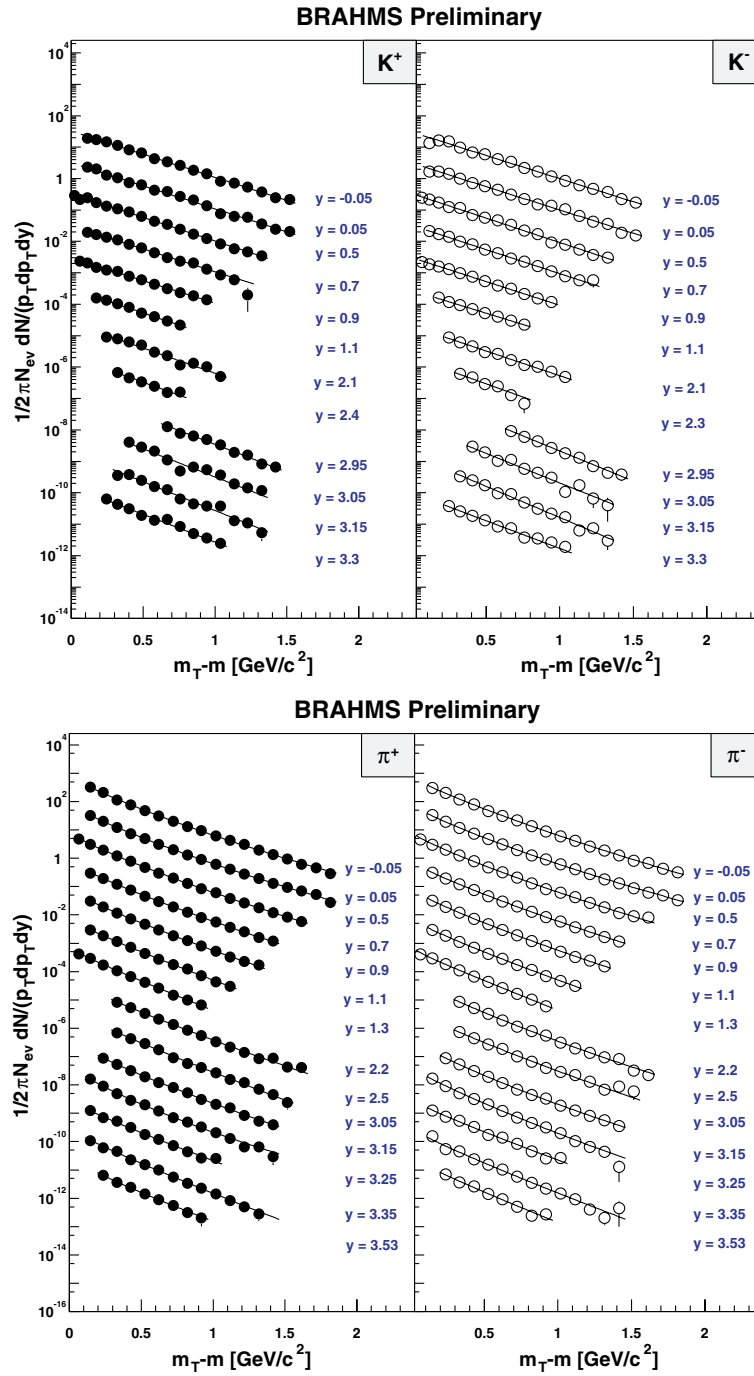


**Figure 1.** The  $m_T$  spectra for kaons and pions for central events (0–5%) at different rapidities. Average rapidities are indicated in the right corner of each spectrum. All spectra are scaled down by successive factors of 10 except the topmost. Solid lines represent  $m_T$  exponential fits to the data for kaons and power-law fits for pions, respectively. Statistical error bars are shown or are smaller than the symbol size.

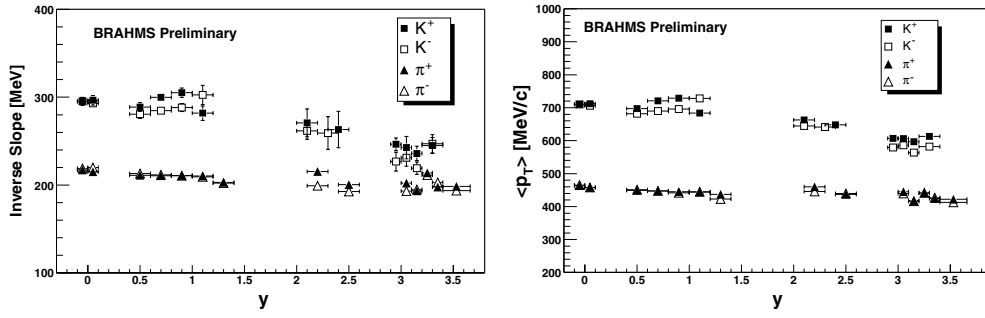


**Figure 2.** Left panel shows kaon and pion slopes obtained from  $m_T$  exponential fits vs rapidity for central events. For pions, the fitting range was chosen between  $0.3 < p_T < 1.0$  GeV/c. The mean values of  $p_T$  for pions and kaons for central events (0–5%) as a function of rapidity is shown in the right panel. Statistical error bars are shown or are smaller than the symbol size.

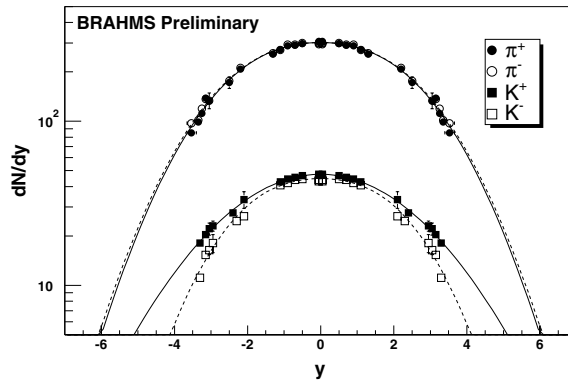


**Figure 3.** The rapidity distributions of  $dN/dy$  for charged pions and kaons in central Au+Au reactions at  $\sqrt{s_{NN}} = 200$  GeV. Measured points in the forward hemisphere ( $y \geq 0$ ) are reflected with respect to mid-rapidity. Solid lines show fits for  $\pi^+$  and  $K^+$  and dotted lines for  $\pi^-$  and  $K^-$ .

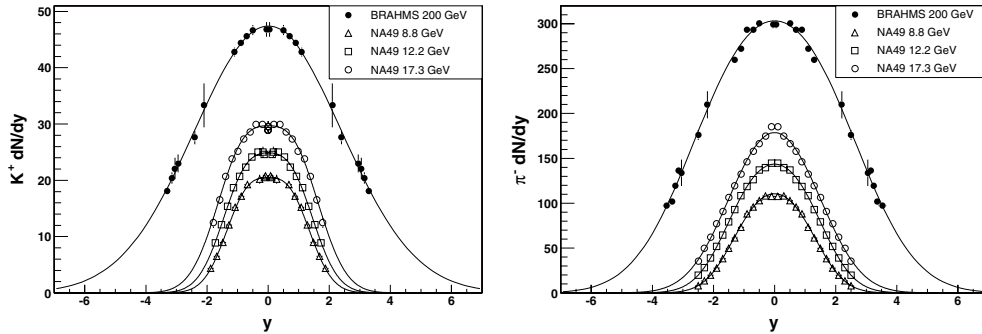


**Figure 4.** Rapidity distributions ( $dN/dy$ ) of  $K^+$  (left panel) and  $\pi^-$  (right panel). BRAHMS preliminary data points are indicated by solid circles. Data from SPS at different energies are shown with open symbols. Measurements for the positive rapidity regions are reflected with respect to mid-rapidity.

While the transverse spectra give insight into the kinetic freeze-out stage of the collision, particle yields and ratios provide information about the chemical freeze-out stage. Particle

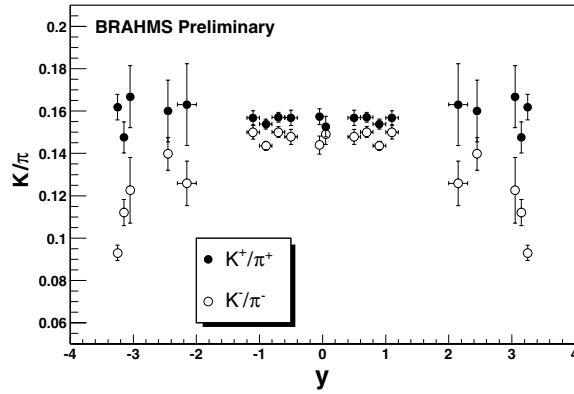


**Figure 5.** Ratios of  $K^+/\pi^+$  (closed symbol) and  $K^-/\pi^-$  (open symbol) as a function of rapidity. Measurements for  $y \geq 0$  are reflected with respect to mid-rapidity. Error bars shown are statistical only.

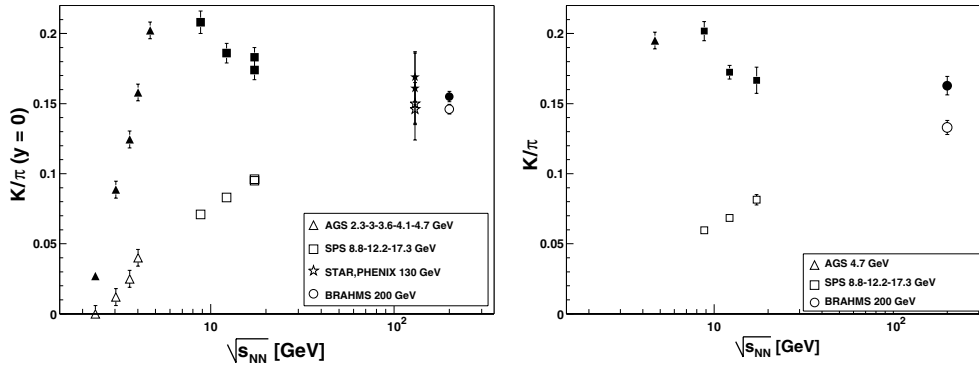


**Figure 6.** Ratios of  $K^+/\pi^+$  (closed symbols) and  $K^-/\pi^-$  (open symbols) yields at mid-rapidity as a function of energy in central Au+Au (Pb+Pb for data from SPS) collisions. Preliminary BRAHMS results are indicated by circles. The ratios integrated over the full phase space are shown in the right panel.

ratios have been analyzed in the context of the grand canonical ensemble with baryon number, strangeness and charge conservation [8]. Figure 7 shows the  $\bar{p}/p$  and  $K^-/K^+$  with curves from statistical calculations. Excellent agreement is found between these calculations and the present measurements. Within grand canonical approach, the near constancy of the temperature for chemical freeze-out found at SPS, at lower RHIC energies, and at the present energy can be thought of as associated with a fixed deconfinement transition temperature and the establishment of chemical equilibrium during hadronization. The small value of the chemical potential indicates a small net baryon density at mid-rapidity. More details can be found in [15].

#### 4. Summary

The BRAHMS Collaboration has measured charged kaon productions as functions of transverse momentum and rapidity. The spectral shape are described well by an exponential in transverse mass for the rapidity range of  $0 \leq y_K \leq 3.3$  with decreasing inverse slopes

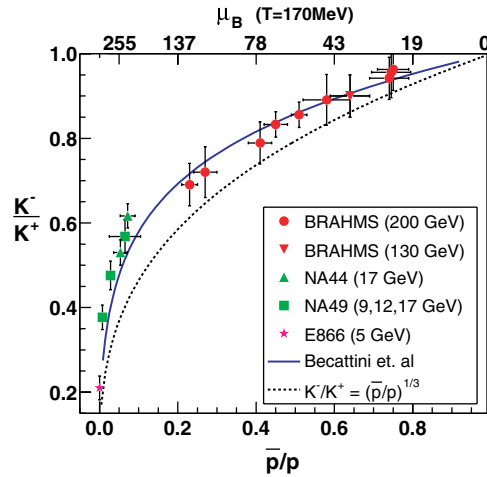


**Figure 7.** Correlation between  $K^-/K^+$  and  $\bar{p}/p$  ratios. Closed symbols represent BRAHMS measurements and open symbols show lower energy data from SPS and AGS. The line shows the calculation by Becattini *et al* [8]. The top scale for the baryon chemical potential  $\mu_B = 3\mu_q$  is in MeV. For the detailed description for the figure, see [15]

and average transverse momentum with measured rapidity. For charged kaon to pion ratios, no significant changes are observed across the measured rapidity range for  $K^+/\pi^+$ , while the  $K^-/\pi^-$  ratio exhibits a significant decrease from  $y \approx 1$  towards higher rapidities. Anti-particle to particle ratios for charged kaons show a strong rapidity dependence which may imply significant interplay between baryonic dynamics and strangeness production at the RHIC energy. The systematics of  $K^-/K^+$  and  $\bar{p}/p$  ratios in the measured rapidity range demonstrates a strongly correlated behaviour which can be described by thermal-statistical models.

No currently available theoretical model successfully reproduces all aspects of strangeness production. Studying the rapidity dependence of strangeness imposes more stringent constraints on theoretical models describing dynamics of nuclear matter created by high-energy heavy ion collisions.

## Acknowledgments

This work was supported by the division of Nuclear Physics of the Office of Science of the US DOE, the Danish Natural Science Research Council, the Research Council of Norway, the Polish State Commission for Scientific Research and the Romanian Ministry of Research.

## References

- [1] Rafelski J 1982 *Phys. Rep.* **88** 331
- [2] Koch P, Müller B and Rafelski J 1986 *Phys. Rep.* **142** 167
- [3] Abbott T *et al* (E802 Collaboration) 1994 *Phys. Rev. C* **50** 1024
- [4] Ahle L *et al* (E866 Collaboration) 1998 *Phys. Rev. C* **58** 3523
- [5] Ahle L *et al* (E866/E917 Collaboration) 2000 *Phys. Lett. B* **490** 53
- [6] Afanasiev S V *et al* (NA49 Collaboration) 2002 *Phys. Rev. C* **66** 054902
- [7] Bearden I *et al* (NA44 Collaboration) 2002 *Phys. Rev. C* **66** 044907
- [8] Becattini F *et al* 2001 *Phys. Rev. C* **64** 024901
- [9] Bleicher M *et al* 2000 *Phys. Rev. C* **62** 061901 and references therein

- 
- [10] Hwa R C and Yang C B 2002 *Phys. Rev. C* **66** 064903 and references therein
  - [11] Adamczyk M *et al* (BRAHMS Collaboration) 2003 *Nucl. Instrum. and Methods A* **499** 437
  - [12] Ouerdane D *PhD Thesis* NBI in preparation
  - [13] Lee J H *et al* (BRAHMS Collaboration) 2003 *Nucl. Phys. A* **715** 482c
  - [14] Bearden I G *et al* (BRAHMS Collaboration) 2002 *Phys. Rev. Lett.* **88** 202301
  - [15] Bearden I G *et al* (BRAHMS Collaboration) 2003 *Phys. Rev. Lett.* **90** 102301
  - [16] Wang X N and Gyulassy M 1991 *Phys. Rev. D* **44** 3501 (<http://www-nsdth.lbl.gov/xnwang/hijing>)
  - [17] Zhang B *et al* 2000 *Phys. Rev. C* **61** 067901